Bulletin of the Seismological Society of America, Vol. 86, No. 6, pp. 1667–1680, December 1996

Analysis of Wave Propagation in the Valley of Mexico from a Dense Array of Seismometers

by Jeffrey S. Barker, Michel Campillo, Francisco J. Sánchez-Sesma, Denis Jongmans, and Shri Krishna Singh

Abstract A dense array of seismometers was installed and operated in the botanical garden of UNAM within the Valley of Mexico during April and May 1994. The slow surface velocities at the array require an approach to array analysis with the capability of measuring arrival-time differences between stations of less than the sampling interval of the data. Applying the method to principal-component seismograms from earthquakes at local and regional ranges from a number of directions provides the first quantitative information on the composition of the wave-field incident upon Mexico City. Phases that propagate through the entire crust, such as the initial *P* and *Lg* waves, cross the array with the expected backazimuth. On the other hand, surface waves in the 2.5- to 5-sec period band, which are sensitive to upper-crustal structure, show systematic rotations of backazimuth. These suggest changes in upper-crustal structure or point scatterers located north and south of Mexico City. For earthquakes outside of the Valley of Mexico, no significant energy was observed propagating across the array from the east (from the lake zone). Thus, although it is clear that seismic waves resonate within the lake zone, little, if any, of this energy is transmitted into the hill zone where the array was located. However, long-duration ground motions are observed at the array, with evidence of multipathing. A back-projection of these late, off-azimuth arrivals indicates that their sources correlate with the boundaries of the Quaternary volcanics of the trans-Mexican volcanic belt.

Introduction

One of the most important problems for seismic zonation is to account for the large variations in ground motion that may occur as a result of topography or near-surface geologic structure: site effects. The primary example of these effects is Mexico City, where the 1985 Michoacan earthquake (over 360 km away) caused extreme damage to 5- to 10-story buildings in an area of the city built on an ancient dry lakebed. Very shortly after the earthquake, it became clear that 1D amplification of ground motion due to the difference in acoustic impedance between the lakebed sediments and the underlying volcanic rocks could not explain the long duration of strong shaking in Mexico City (Sanchez-Sesma *et al.*, 1988; Kawase and Aki, 1989). Bard *et al.* (1988), Sanchez-Sesma *et al.* (1989), Campillo *et al.* (1988), and Kawase and Aki (1989) modeled the 2D response of the basin due to an incident plane wave and found that edge-generated surface waves prolong the resonance of the basin, particularly in the presence of a thin, soft clay layer. However, Chavez-Garcia and Bard (1994) have shown that with a reasonable estimate of anelastic attenuation for the clay layer ($Q_s = 25$), surface waves with significant amplitudes are generated near the edge of the basin but cannot propagate very far into the lakebed zone. An alternative explanation, offered by Flores *et al.* (1987), Seligman *et al.* (1989), and Mateos *et al.* (1993), is that the long duration is due to the lateral resonance of horizontally propagating *P* waves, which are generated by *S*-to-*P* conversion upon entering the clay layer and are not affected by the low shear-wave *Q* of the clay. Chavez-Garcia and Bard (1994) and Sanchez-Sesma and Luzon (1996) argued that the horizontal amplitude of the *S*-to-*P* conversion is very small, that if it exists, the frequency of this resonance is much lower than the nearly harmonic 2-sec ground motion observed in the lake zone, and that higher modes of resonance actually correspond, once again, to Rayleigh waves.

As a result of geotechnical measurements of shallow surface geology, the Valley of Mexico has been divided into three seismic hazard zones (see Fig. 1): (I) the hill zone, with volcanic flows and tuffs at the surface; (II) the transition zone, with Quaternary alluvium; and (III) the lake zone, with 10 to 100 m of clay underlain by sand. Spectral ratios suggest that ground motions in the lake zone are amplified by factors up to 50 relative to the hill zone for frequencies from 0.2 to 0.7 Hz (e.g., Singh *et al.*, 1988). Ordaz and Singh

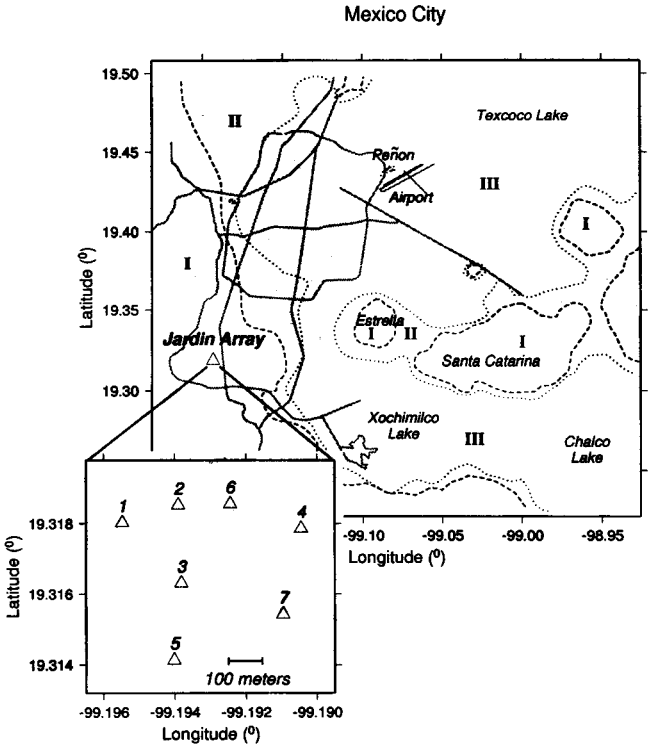

Figure 1. Map of Mexico City showing seismic zones I (hill zone), II (intermediate zone), and III (lake zone). Highways and other landmarks are shown in gray. The location and geometry (inset) of the Jardin array are also shown.

(1992) and Singh *et al.* (1995) have shown that ground motions in the hill zone are, themselves, amplified by a factor of about 10 at the same frequencies relative to ground-motion attenuation curves established outside of Mexico City. Singh and Ordaz (1993) demonstrate that if the triggered seismographs in the hill zone measure a sufficient length of record (unlike accelerograms of the 1985 Michoacan and 1989 Guerrero earthquakes), 1D propagators applied to these records can reproduce the duration of strong shaking in the lake zone. Thus, they suggest that the long coda observed in the lake zone is already present in the coda of the hill zone (but at lower amplitude) and that beating in the coda must be due to multipathing between the source and the hill zone or within the volcanic layers of the hill zone. In a comment, Baez *et al.* (1994) remind Singh and Ordaz (1993) to consider feedback into the hill zone from the lake zone (in particular, their *P*-wave resonance model). Bard and Chavez-Garcia (1993) have also demonstrated that applying a 1D propagator to ground motions computed from a 2D sediment model yields unrealistically long durations relative to a complete 2D model, including the clay layer above the sediments. Of course, the volcanic layer of the hill zone has perhaps an order of magnitude greater extent (both horizontally and vertically) than the sediment layer modeled by Bard and Chavez-Garcia (1993).

In this study, we present the first results from a dense array of seismographs placed within the Valley of Mexico in order to analyze the wave-field incident from a number of directions. Recently, dense, temporary arrays have been deployed to measure weak motions in a number of areas (Frankel *et al.*, 1991; Hartzell *et al.*, 1994; Mori *et al.*, 1994; Lee *et al.*, 1994; Spudich *et al.*, 1996). In most of these studies, correlation techniques and polarization analysis are used to identify secondary, off-azimuth arrivals. In the case of Mexico City, low surface velocities result in nearly vertical incidence angles, and the small aperture results in very small arrival-time differences as the waves cross the array. Beamforming and *f-k* analysis yield poor resolution of the horizontal slowness vector. Therefore, we use a procedure that allows accurate determination of arrival-time differences less than the sampling rate of the data. The method is applied to earthquakes north, northeast, southeast, and south of Mexico City.

The Jardin Array

An array of 7 three-component seismometers was installed and operated from 1 April to 14 May 1994 within the botanical garden ("jardin" in both Spanish and French) of the Universidad Nacional Autónoma de México (Fig. 1). The array was located in the hill zone (seismic zone I), near the edge of the intermediate zone (seismic zone II), on the western edge of the Valley of Mexico. Of course, it would have been desirable to record ground motions in the lake zone (seismic zone III), but the high level of ambient cultural noise within zones II and III within Mexico City precluded collecting useful data during the time period of this experiment. Also, we wished to test the conclusions of Singh and Ordaz (1993). Therefore, the array was placed in a relatively quiet area of zone I. The instruments were buried or placed on slabs near identifiable landmarks (a greenhouse, storage buildings, parking lots, private access roads). Standard and GPS surveys were performed to locate the stations both horizontally and vertically. Later, the locations were checked using aerial photos and large-scale maps. The locations are listed in Table 1. The aperture of the array is about 500 m in both N–S and E–W directions with an average station spacing of about 150 m.

The instruments of the array are part of the portable LITHOSCOPE network (Poupinet *et al.*, 1990). Each station consists of a three-component, 5-sec Lennartz velocity transducer digitized continuously with 16-bit sampling at a rate of 25 samples per second. The internal clock at each station was calibrated by means of a GPS receiver every two days, and Campillo *et al.* (1994) demonstrated that the clock drift was quite linear with errors less than about 0.2 sec/day. Nevertheless, in the analysis procedures described below, more accurate time corrections are determined for each event recorded. The orientation of the horizontal components was measured in the field.

Over 24 well-located events were recorded during the

Table 1
Jardin Array Station Locations

Station	Latitude (°N)	Longitude (°W)	Relative Position (*m* E)	(*m* N)	(*m* Up)	Location
1	19.318	99.19548	−157	−55.6	0.86	grande serre tropicale
2	19.3185	99.1939	0	0	0	petit local
3	19.3163	99.19382	8.3	−246	1.92	tunnel
4	19.3179	99.19045	342	−74	1.26	heliport
5	19.3141	99.19402	−11.4	−498	5.9	seminaire
6	19.3186	99.19245	143.8	3.8	−2.87	serre blanche
7	19.3154	99.19096	291.4	−345	1.94	jungle

array deployment (Fig. 2). Most were located along the Mexican subduction zone, primarily from the area of the Guerrero seismic gap (magnitudes 3.9 to 4.9). However, two deep earthquakes from southern Bolivia (magnitudes 5.8 and 6.2) were recorded, as were small events from the north, northeast, and southeast. Figure 3 shows an example of the radial component of ground velocity at each station for the Guerrero event of 14 May (0653 GMT, magnitude 4.9). Due to the small aperture of the array, the ground motions are quite coherent from one station to another, but slight variations are apparent. It is these differences between the waveforms that allows us to identify the type and direction of propagation of various waves crossing the array through time. We have selected 11 events at local and regional distances for analysis (Table 2; black stars in Fig. 2) to identify scatterers and sources of reverberation within and around the Valley of Mexico.

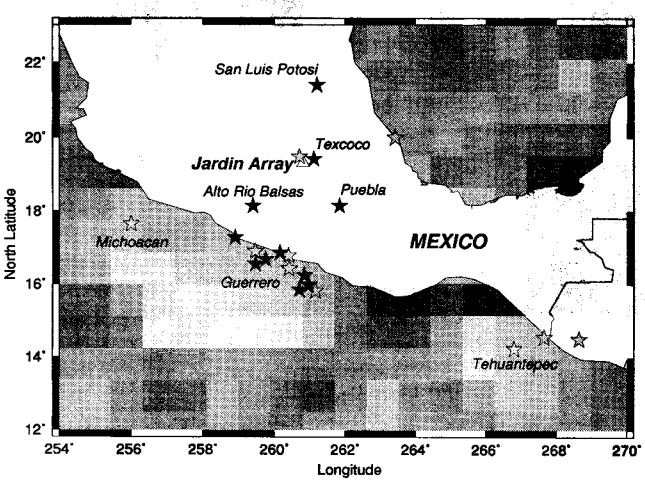

Figure 2. Map of Mexico showing the Jardin array (triangle) and earthquakes recorded during the array deployment (stars). Events analyzed in this study are indicated by black stars.

Array Processing and Analysis

In Mexico City, the resonant period of the long-duration response of the valley is 2 to 5 sec, considerably longer than that encountered for the other arrays mentioned above. A complicating factor is that the near-surface velocity is so low (the near-surface *P*-wave velocity at the botanical garden was measured as 0.55 km/sec; Campillo *et al.,* 1994) that body waves arrive nearly vertically beneath the array. Because of the sampling rate of the data, initial analyses using the grid-search method of Frankel *et al.* (1991) resulted in a broad peak in cross-correlation centered slightly away from but encompassing a slowness value of zero. Nearly identical results were obtained using the *f*-k analysis functions in the SAC package (from Lawrence Livermore Labs) and a frequency-domain beamforming program by Olivier Coutant (personal comm.). Each of these approaches was tested using synthetic seismograms and operates correctly. However, when synthetics with slow surface velocities and the same sampling rate as the Jardin array were used, none could resolve backazimuth (the direction from the receiver to the source) adequately. The application to Mexico City requires a method with resolution of arrival-time differences smaller than the sampling interval of the data.

The array analysis procedure combines array-averaged polarization analysis, a method for measuring the time delay between stations by a linear regression on the phase difference spectrum, and linear inversion of these time delays for the horizontal slowness of a plane wave. The polarization analysis makes use of all three components of ground motion and, because of the array average, gives a fairly robust measure of ground motion within the array. However, it is not sensitive to the differences in ground motion across the array, and it is these differences that indicate the direction and speed of wave propagation. The phase difference slowness inversion, on the other hand, is sensitive to these differences but gives separate estimates of wave propagation for each of the three components. It is also less stable and more susceptible to the effects of noise and errors in the data. Our solution is a combined approach that takes advantage of the strengths of both of these methods.

We first bandpass filter the data into a series of octave-width bands with periods of 0.3125 to 0.625, 0.625 to 1.25, 1.25 to 2.5, 2.5 to 5.0, and 5.0 to 10.0 sec. The *Pg* and *Lg* wave trains are contained primarily in the first three bands, but the later arriving, long-duration ground motion, like that which caused much of the damage in the 1985 Michoacan

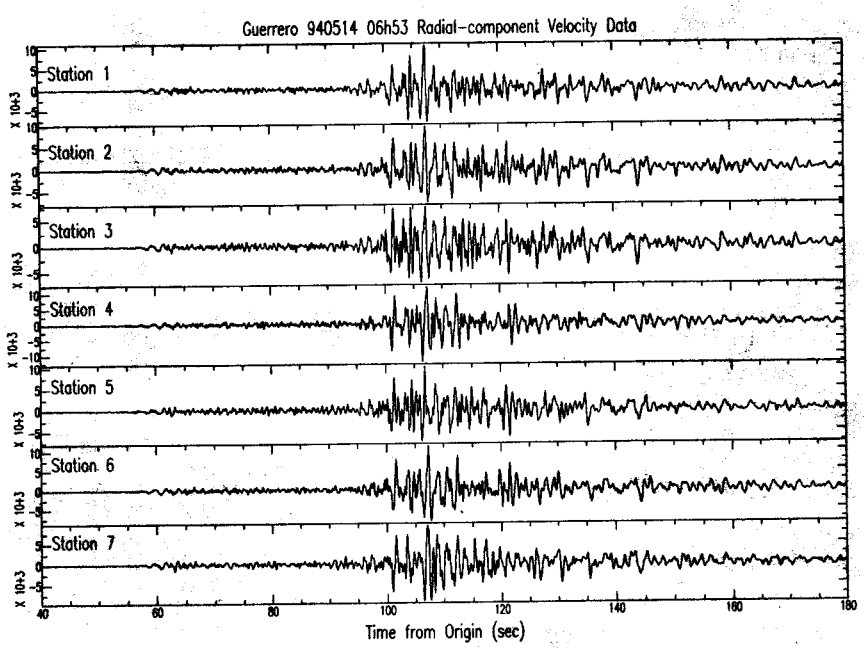

Figure 3. Radial (North) component ground velocity data recorded at the seven stations of the Jardin array for the Guerrero earthquake of 14 May (06h53) 1994.

Table 2
Earthquakes Recorded at the Jardin Array*

No.	Origin Time (GMT) Date	HrMn	Sec	Dist (km)	Azim (°)	BAZ (°)	Mag	Depth (km)	Location
1	4/22	0620	25.1	198.1	48.6	229.1	4.1	69	Alto Rio Balsas
2	4/30	0810	29.5	34.0	251.0	70.9	4.2	1.5	Texcoco
3	5/4	1957	52.0	280.7	14.2	194.4	4.4	31	Guerrero
4	5/5	1218	50.7	337.4	24.6	205.0	4.4	41	Guerrero
5	5/5	1239	29.6	312.6	20.8	201.1	3.9	43	Guerrero
6	5/6	2109	35.0	169.4	320.5	140.2	4.9	70	Puebla
7	5/10	0242	25.0	303.2	41.6	222.2	4.2	9	Guerrero
8	5/11	0508	41.2	235.0	190.2	10.0	4.0	15	San Luis Potosi
9	5/14	0653	11.8	340.7	359.6	179.5	4.9	19	Guerrero
10	5/14	0659	49.7	384.0	1.80	181.8	4.6	18	Guerrero
11	5/14	0736	33.9	369.8	357.5	177.4	4.6	20	Guerrero

*Locations and origin times are from the catalog of the Instituto de Geofísica, UNAM.

earthquake, appears in the fourth band (2.5 to 5 sec). Because of the instrument response, there is little energy in the longest-period band. Similarly, the two shorter-period bands include predominantly random scattered energy. Thus, most of the useful information is contained in the 1.25- to 2.5- and 2.5- to 5-sec bands. Time windows are chosen short enough to enable a detailed analysis and to minimize mixing of multiple arrivals within a single window but long enough to encompass the passband of the data. This typically means time windows twice the length of the longer-period limit of the passband (e.g., 10 sec for the 2.5- to 5-sec band). The time windows are overlapped by 75%, and we interpret the results in terms of groups of time windows rather than in terms of individual windows.

In the polarization analysis, we use a time-domain eigenvalue method based on Jurkevics (1988). For a given station, the three components of ground motion are windowed and rotated into the coordinates x_i (i = 1, 2, 3 = east, north, up). Within each window, the covariance matrix is computed as $S_{ij} = \Sigma x_i x_j / N$, where N is the number of points within the time window. To make full use of the fairly coherent data across the array, we compute the array-averaged covariance matrix as $\overline{S_{ij}} = \Sigma S_{ij}/M$ for M stations. Since the time windows chosen are typically several seconds in length (or at least several tens of the sampling interval), and the time lags due to waves crossing the array in Mexico City are often a fraction of the sampling interval, we make no correction for phase propagation before taking the array average of the covariance matrix. Besides, at the time the polarization analysis is performed, those waves have not yet been interpreted.

An eigenvalue decomposition of the 3 × 3 covariance matrix results in the three principal components of ground motion within the time window. P waves, S waves (in the absence of anisotropy), and Love waves are expected to generate a single, nonzero eigenvalue, since their particle mo-

tion is polarized in a single direction. Rayleigh waves generate two nonzero eigenvalues, since their particle motion is elliptical within a vertical plane. In general, however, since there is noise and multiple arrivals may interfere within a given window, all three eigenvalues will typically be nonzero. Since our purpose is to identify a single plane wave propagating across the array within each time window, we interpret only the largest eigenvalue, λ_1; its eigenvector u_i indicates the direction of particle motion for this wave. The inclination and azimuth of that particle motion are given by

$$i = \tan^{-1} \frac{\sqrt{u_1^2 + u_2^2}}{u_3} \text{ and } Az = \tan^{-1} \frac{u_1}{u_2}.$$

There is a 180° ambiguity in particle motion direction, so we consider only $0 < i < 90°$ and $0 < Az < 180°$. For a P wave, the inclination of particle motion is the apparent incidence angle, which is related to the actual incidence angle of the ray through the ratio of P- and S-wave velocities. Bockelmann (1995) shows that the difference is small for ray incidence angles less than about 60°, so in the case of Mexico City, we can ignore the distinction. Although the linearity or planarity of the particle motion may be determined from ratios of the eigenvalues, we prefer to plot both the amplitude of the largest eigenvalue, λ_1, as well as the total amplitude, $\sqrt{\lambda_1^2 + \lambda_2^2 + \lambda_3^2}$, for each time window. When these are similar, a single plane wave is a good approximation of the incident wave field. Before applying the next step, we rotate the three-component ground-motion data for each window into the single principal-component direction. This improves the signal-to-noise ratio as well as the interstation coherence. To ensure that the time windows for all stations begin at the same time, the seismograms are linearly interpolated to the same absolute time sampling before windowing and rotation.

To determine the time delay between stations, we use a method developed by Poupinet *et al.* (1984) for analysis of earthquake doublets. The principal-component seismograms at each station are windowed and tapered [$S_1(t)$ and $S_2(t)$] then Fourier transformed [to $F_1(\omega)$ and $F_2(\omega)$], and the cross spectrum is formed [$C_{12}(\omega) = F_1(\omega)^* F_2(\omega)$, where * denotes the complex conjugate]. The time delay is determined by a linear regression on the slope of the phase of the cross spectrum ($\varphi(\omega) = \tan^{-1} Im\{C_{12}(\omega)\}/Re\{C_{12}(\omega)\}$), with a weighting function determined by the power and coherence between signals:

$$W(\omega) = \sqrt{\sqrt{C_{12}(\omega)}/[\text{coh}(\omega)^{-2} - 1]},$$

where

$$\text{coh}(\omega) = \frac{|C_{12}(\omega)|}{|F_1(\omega)||F_2(\omega)|}.$$

Thus, the linear regression over n points between specified frequencies is

$$\Delta t = \frac{\sum_n \omega_i \phi_i W_i^2}{\sum_n \omega_i^2 W_i^2}$$

with the additional constraint that the line pass through the origin. The weighting factor minimizes the influence of frequencies for which there is little power or coherence between signals. Padding the windowed time series before Fourier transforming increases the effective sampling rate in frequency (although without any increase in information), so that the linear regression can be taken over several (usually tens of) frequency points. If the time delay is greater than the sampling interval of the data, the seismograms are lagged by an integral number of samples, and the regression is repeated. Thus, the final regression always determines the portion of the arrival-time difference that is a fraction of the sample interval. Tests with data and synthetics indicate that it is important to choose the frequencies for the regression carefully but that time delays substantially less than the sampling interval of the data may be reliably obtained.

Once the time delay between each pair of stations has been determined for a given time window, we may solve for the slowness of the assumed plane wave propagating across the array. Since for the Jardin array there is very little elevation difference between stations, the vertical component of slowness is poorly resolved, and we solve only for the horizontal slowness. If the known station separations are Δx and Δy (x east and y north), the predicted time delay between station pair i is $\delta t_i = p_x \Delta x_i - p_y \Delta y_i$. The partial derivative of δt_i with respect to p_x is simply $-\Delta x_i$, while that with respect to p_y is $-\Delta y_i$. It is simple matter to invert the difference between the observed and predicted time delays ($\Delta t_i - \delta t_i$) for the change in slowness from the starting model, Δp_x and Δp_y. We use a generalized inverse, but since this is a linear problem and both parameters are resolved, it is equivalent to a simple, undamped least squares.

Before inverting for slowness, it is important to take account of any timing errors in the data. We may consider that for a given event, each station has a constant but unknown time error, E_j, which when combined with the errors from other stations, yields an error in the time delay estimate for each pair of stations, ε_i. We assume that we know the direction and phase velocity of the initial P wave, so we may predict the time delay for this wave. Note that we could choose any wave for this calibration, but the initial P wave is least ambiguously identified, and because of its near-vertical incidence, the predicted time delays are relatively insensitive to the assumed backazimuth. The difference between the observed time delay for this window and the predicted time delay gives an estimate of the time delay error: $\varepsilon_i = (\Delta t_i^0 - \delta t_i^0)$. These are determined from the unfiltered velocity data so as to provide the broadest frequency band for the linear regression of the phase difference. The errors in the time delays are determined for each pair of stations, so if there are N stations each with absolute time error E_j, there will be $N - 1$ time-delay errors that depend on this absolute error. With simple matrix algebra, we may

determine $N - 1$ estimates of the absolute time error for each station, E_j (assuming that one of the stations has zero error), which we average to determine the station time correction. Since the station time corrections should be constant between time windows and frequency bands for a given event, these are stored in a file and applied when the seismograms are windowed for rotation into the principal component. Slight errors in the phase velocity and backazimuth assumed in the calibration will result in slight, systematic errors in the inverted slowness; however, test inversions indicate that the relative slownesses are quite stable.

Synthetic Tests

As an example and test of the analysis method, synthetic seismograms were computed using the frequency-wavenumber integration method of Barker (1984) for a simple continental crustal model with two layers over a half-space. The array geometry of the Jardin array was assumed, and the source was located at a depth of 10 km, 273 km away at a backazimuth of 190°, and a mechanism appropriate for a subduction zone earthquake. The synthetics were computed with a sampling rate of 10 samples per second but, to be consistent with the Jardin array data, were interpolated to 25 samples per second. Nevertheless, the original Nyquist frequency (5 Hz) imposes an upper limit on the frequency band for this test. To test the determination of station time errors, the start times of the synthetics were shifted by -0.08, 0.16, -0.24, 0.32, -0.40, 0.48, and -0.56 sec for stations 1 through 7, respectively. The station time corrections were determined for the time window centered at 45 sec in the broadband (unfiltered) synthetics. From the polarization analysis, we fix the slowness for this window to correspond to a phase velocity of 8.0 km/sec and a backazimuth of 190°. The resulting time errors, assuming that station 2 has zero error, are -0.241, 0.0, -0.406, 0.160, -0.571, 0.320, and -0.726 sec for stations 1 through 7, respectively. If we add the known error for station 2 (0.16 sec), the results give the correct values to within 0.01 sec. The results are shown for the synthetics, bandpass filtered from 1.25 to 2.5 sec, in Figure 4. For this figure, and following similar figures, the three components of ground motion at one of the stations is shown at the top. The three plots below this present the array-averaged polarization analysis, with particle motion azimuth and inclination in degrees, the amplitude of the largest eigenvalue (solid dots) and the total amplitude (open dots) for each time window. The dots are plotted at the center of each time window, and each window overlaps its neighbor by 75%; horizontal bars plotted on the first dot indicate the time window duration. The theoretical radial direction is denoted by a dashed line on the plot of azimuth, and we see that the *P*-wave train has its particle motion in this direction. The lower three plots present the results of the inversion for horizontal slowness. Shown are the phase velocity (the inverse of the length of the horizontal slowness vector), the backazimuth (the direction from which the wave propagates across the array), and the root-mean-squared error, shown as the

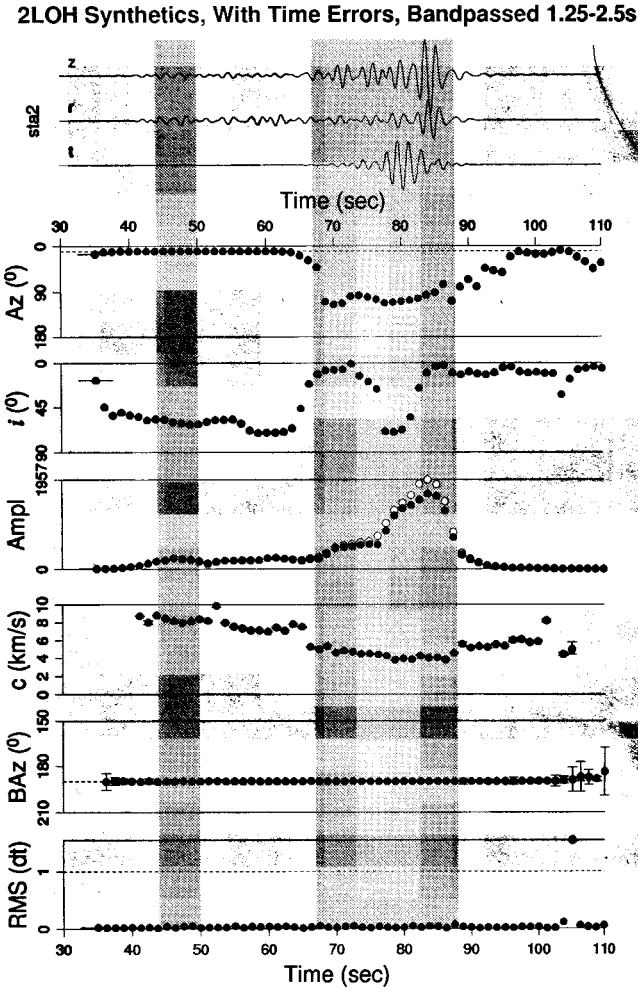

Figure 4. Array analysis results for synthetic ground velocity seismograms for a two-layer over half-space model. Known time errors have been included in the synthetics in order to test the determination of station time corrections. Shown at the top are representative three-component seismograms, bandpass filtered from 1.25- to 2.5-sec period. The three plots below this show the results of the array-averaged polarization analysis, showing the azimuth, inclination, and amplitude of the largest eigenvalue of ground motion (solid dots) within each time window. The total amplitude is shown as open dots in the third plot, and the theoretical radial direction is indicated as a dashed line in the first plot. The bottom three plots show the results of the inversion of time lags for horizontal slowness. Shown are the phase velocity (the inverse of the length of the horizontal slowness vector), the backazimuth (the direction from which the wave crosses the array), and the root-mean-squared error plotted as a fraction of the data sampling interval. Once again, the theoretical backazimuth is indicated as a dashed line. The dots are plotted at the center of each time window, the duration of which is indicated by horizontal bars plotted for the first time window. Error bars indicate the formal errors in the inversion (one standard deviation in each component of slowness). Shading emphasizes arrivals discussed in the text.

fraction of the sampling interval, *dt*. Vertical bars indicate the formal errors in the inversion (one standard deviation in each component of slowness) due to phase regression errors. These are quite small, and as discussed below, do not represent all of the error in the analysis. Once again, the theoretical backazimuth direction is denoted by a dashed line. In the time windows for which there is significant signal, the slowness inversion gives the correct backazimuth (within 1° or 2°), and the phase velocities are consistent with the model. Note that since the time errors that were added were not random, inversion without adequate station time corrections would result in solutions systematically offset from the correct ones.

A second synthetic test is shown in Figure 5. In this case, we have added random (white) noise equal to 5% of the maximum amplitude in the time domain to the original synthetics. The noise is uncorrelated between traces, and as in real data, the actual signal-to-noise ratio varies for different time windows and different frequency bands. Once again, station time corrections were determined from the *P*-wave window (centered at 45 sec) on the broadband synthetics. The results were near zero (the correct value), ranging from -0.0030 to $+0.0028$ sec (less than 1/10 of the sampling interval). Figure 5 shows the results for the synthetics, bandpass filtered from 1.25 to 2.5 sec. The polarization analysis is essentially unaffected by the addition of noise (compare Figs. 5 and 4). The phase velocity is fairly stable for time windows with significant amplitude. However, the addition of noise causes a variation in the determined backazimuth of about 5° to 10°. Of course, where there is little signal above the noise level in this frequency band, such as late in the *P* coda and beyond 90 sec, the RMS error is relatively large and the determination of the slowness vector is unstable. This test indicates that, in the presence of noise, the determination of backazimuth for time windows with significant signal in the frequency band of interest has a limit of accuracy of 5° to 10°, even though the formal errors in the inversion indicate a greater accuracy.

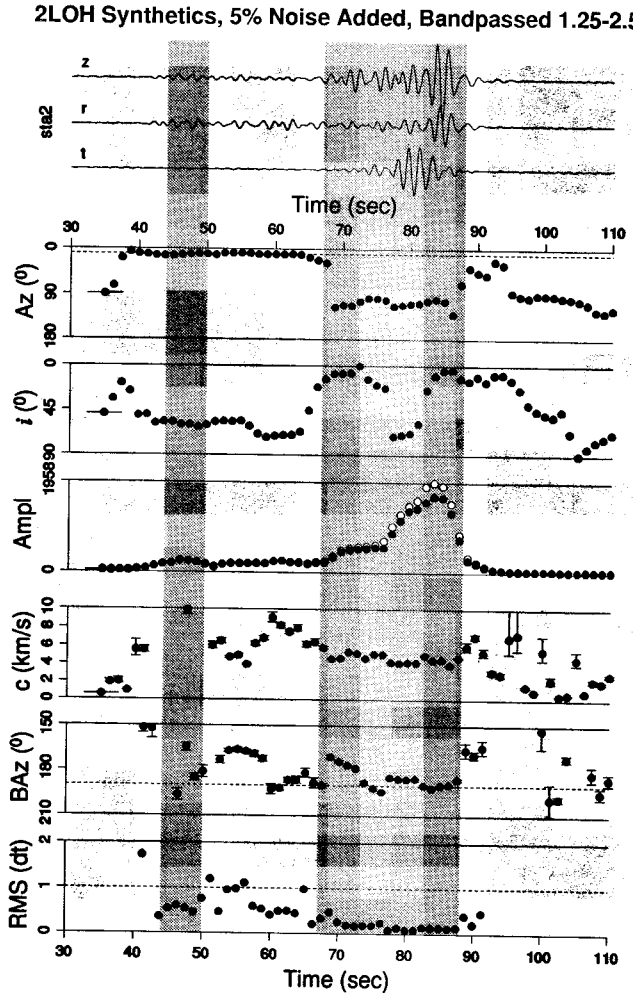

Figure 5. Array analysis results for the synthetic seismograms that include uncorrelated random noise with a level of 5% of the peak time-domain amplitude. This illustrates the expected level of variation of results in the presence of noise and the instability of the inversion when the signal-to-noise ratio is very low. Note that the variation due to noise is greater than the formal errors in the inversion. Same format as Figure 4.

As a third synthetic test, we wish to identify off-azimuth arrivals in a laterally varying velocity structure. We use synthetics computed by Pedersen *et al.* (1995) using an indirect boundary element method for a 2D sedimentary basin with a single plane wave obliquely incident from below. The model consists of a N-striking sedimentary valley of width 10 km, depth 0.5 km, and shear velocity 1.1 km/sec over a half-space with shear velocity 2.8 km/sec. Ground-velocity impulse-response synthetics were computed for positions at 100-m increments across the valley (an E–W line), low-pass filtered at 1.6 Hz, then interpolated to a sampling rate of 25 samples per second. An example for the case of an *SV*-wave incident from an azimuth of $-60°$ and an incidence angle of 60° is shown in Figure 6. To simulate the Jardin array geometry, we select synthetics with appropriate station separations in the x direction (E–W), then apply a constant time shift for each record to simulate station separation in the y direction (N–S). The time shift, $\Delta t = -\Delta y/c_y = -\Delta y \sin(i) \sin(Az)/V$, is determined by the y component of the phase velocity, c_y, of the incident wave in the substrate below the valley, which depends on the velocity in the substrate, V, the incidence angle, i, and the azimuth, Az, measured clockwise from the $-x$ direction. Figure 7 shows the array analysis applied to the synthetics shown in Figure 6 if the "array" is placed 4 km from the western margin of the valley. In this case, we show unfiltered synthetics, but the frequency band of the analysis is from 0.5 to 1.5 Hz. The direct wave arrives at about 4 sec (highlighted in gray), and the polarization has the expected azimuth and inclination for an *SV* wave. In the slowness inversion, we see that the direct wave arrives from the expected backazimuth ($-60°$ from N) and with an appropriate phase velocity. At about 8 sec, the particle motion

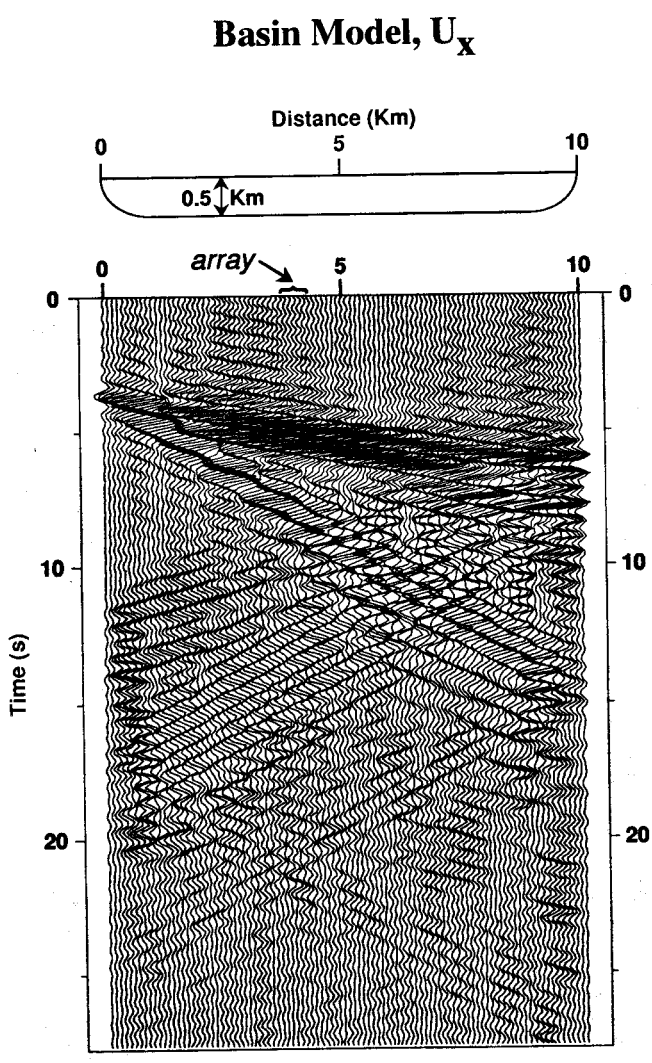

Figure 6. East-component synthetic ground velocities along an E–W profile across a N-striking sedimentary valley, computed with the indirect boundary element method of Pedersen *et al.* (1995) for an *SV*-wave incident at 60° from a backazimuth of −60° (WNW). The position chosen for the array analysis is indicated at the top of the seismograms.

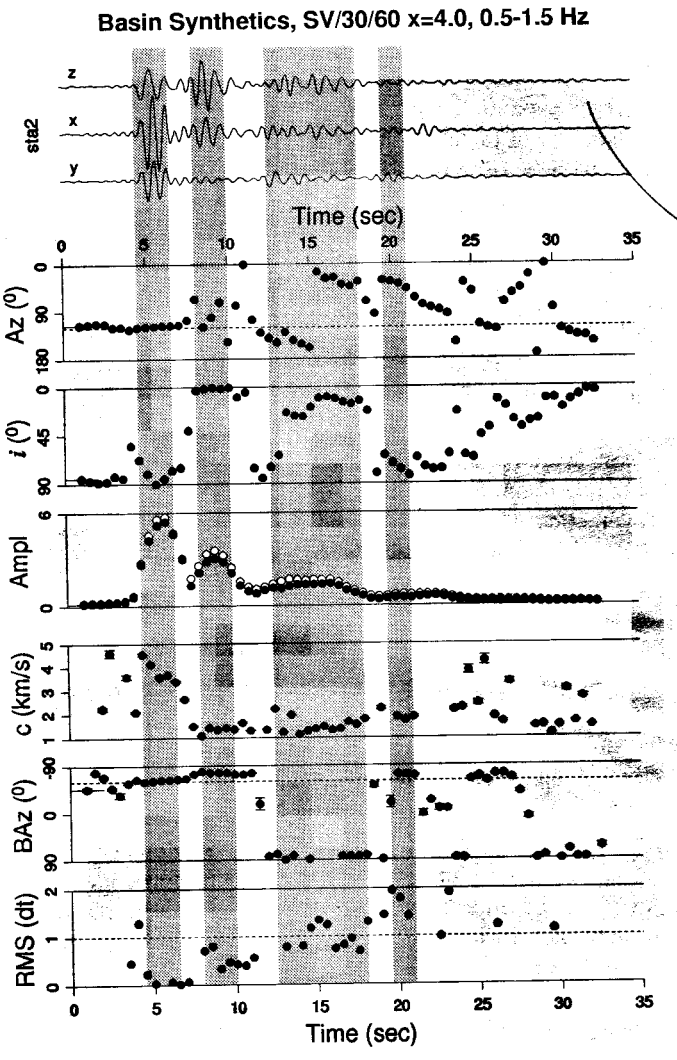

Figure 7. Array analysis of the unfiltered synthetic ground velocities computed 4 km from the edge of a N-striking sedimentary valley for an *SV*-wave incident from a backazimuth of −60°. Same format as Figure 4.

becomes nearly vertical, the phase velocity decreases, the backazimuth shifts toward the west, and the particle motion shifts toward the east. This is the Rayleigh wave generated from the western edge of the valley and may be seen in Figure 6 as the second-arriving wave that propagates slowly from west to east. At 12 to 13 sec, the backazimuth abruptly changes to the east (slightly less than 90°), the particle motion rotates from southeast to south, then to northeast, and the inclination varies from near horizontal to near vertical. This is the combination of Love and Rayleigh waves generated at the eastern margin of the valley. At later times, multiple reflections of these edge-generated surface waves interfere, and while it is difficult to distinguish specific arrivals in the synthetic seismograms (Fig. 6), the backazimuth of the slowness inversion oscillates from west to east. This test shows that the array analysis method is capable of distinguishing multiple arrivals propagating across the array from different directions through time, for the case of a single incident plane wave. This is precisely what we wish to determine for Mexico City, but of course, in that case, the incident wave field is much more complex.

Results

Although the source region of greatest seismic risk for Mexico City is the subduction zone to the south, we will begin with the results for a small earthquake from the north, in the region of San Luis Potosi (magnitude 4.0; see Fig. 2 for location). Although the signal-to-noise ratio is relatively low, the *P* wave may be identified in the 1.25- to 2.5-sec

band (Fig. 8a) at about 35 sec, with particle motion close to vertical (inclination 15°) and in the expected direction (the theoretical backazimuth is 10°). The station time corrections determined for this phase from the unfiltered data are all less than 0.045 sec (see Table 3 for the station time corrections for each event analyzed), and we see that the formal errors and the RMS time errors for the slowness inversions are small for time windows with significant arrivals. Upon arrival of the *Lg* phase beyond about 65 sec, the particle motion becomes horizontal and largely in the radial direction. The phase velocity steadily decreases from a very high phase velocity for the initial *S*-wave arrival (5 to 6 km/sec) to more typical values of 1.5 to 3 km/sec; however, the backazimuth also systematically rotates to the north (at 68 to 85 sec) and to about 60° west of north beyond 90 sec. Late-arriving, long-period surface waves are better seen in the 2.5- to 5-sec band (Fig. 8b). The principal component of motion consists of Rayleigh waves at 90 sec, changes to a mixture of Love and Rayleigh waves at 97 sec, and back to Rayleigh at 110 sec. The initial arrival at 90 sec crosses the array with a backazimuth close to that expected, but later arrivals are rotated 20° to 30° toward the NNW. From these two bands, we see that the *P* wave and the initial *S* and Rayleigh waves cross the array from the expected direction, but the *Lg* coda and the surface-wave arrivals appear to be coming from the northwest. This indicates forward scattering or refraction from a location north to northwest of the array. We see no significant energy propagating across the array from the east, the direction of the lake zone.

A relatively deep earthquake (70 km) beneath Puebla (magnitude 4.9; once again, see Fig. 2 for location) provides information on wave propagation from a well-located onshore earthquake from the southeast. *P* waves are not strong in the 2.5- to 5-sec band (Fig. 9), but the first *S* wave arrives

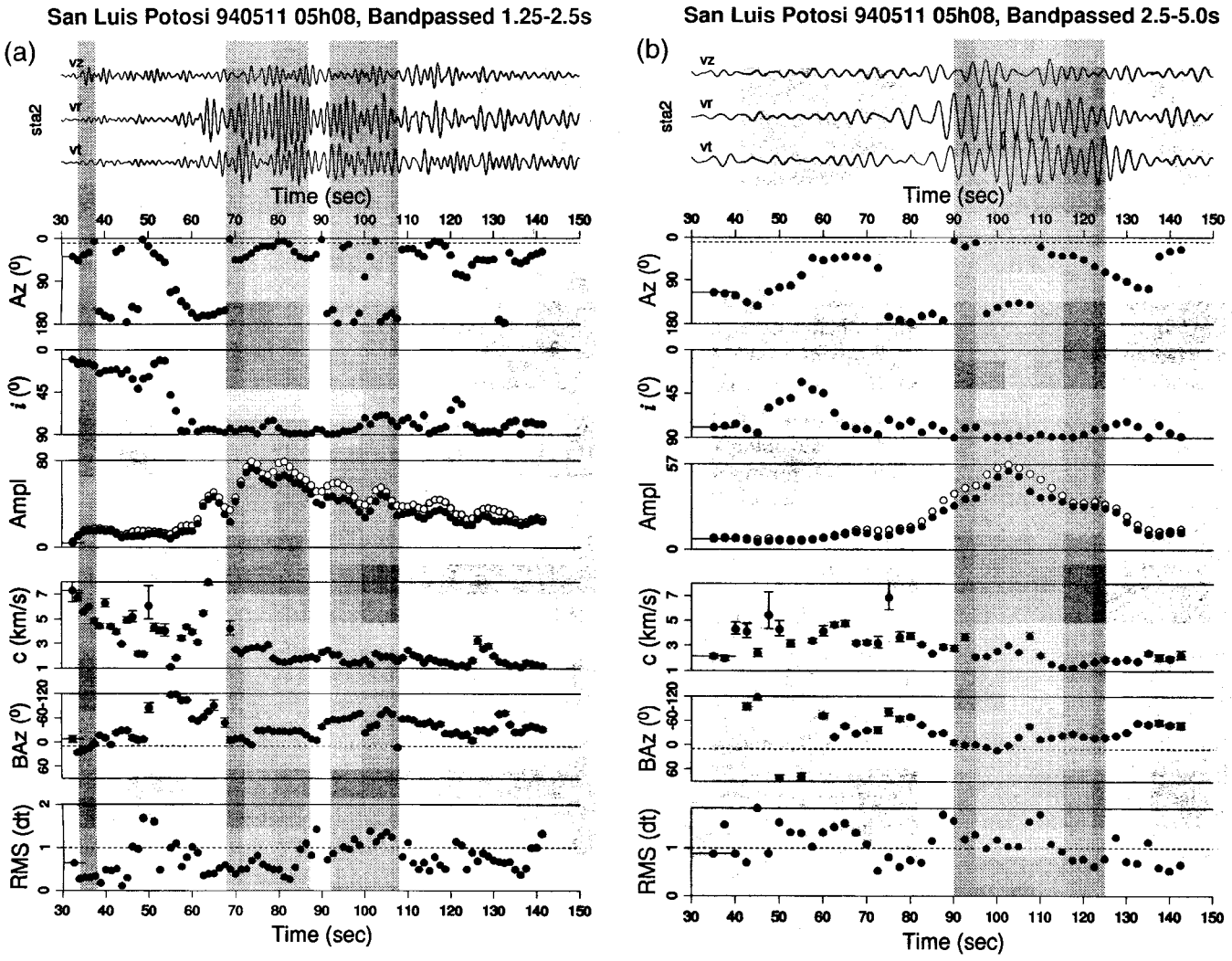

Figure 8. (a) Array analysis results for the observed ground motions from the San Luis Potosi earthquake bandpassed from a 1.25- to 2.5-sec period. Same format as Figure 4. (b) Array analysis results for the observed ground motions from the San Luis Potosi earthquake bandpassed from a 2.5- to 5-sec period. Same format as Figure 4.

Table 3
Station Time Corrections

No.	Time (sec)	Freq. (Hz)	c (km/sec)	BAZ (°)	Station Time Corrections (sec) 1	2	3	4	5	6	7
1	27.0–32.0	0.2–1.0	10.	230.	0.026	0	0.300	0.133	0.042	−0.110	−0.012‡
2	6.5–9.0	0.5–1.0	10.	70.	0.019	0	−0.012§	−0.015	0.028	0.779	−0.043
3*	35.0–40.0	0.5–1.5	10.	194.	−0.006	0	0.156	0.029	−0.057	−0.155	0.037
4*	42.5–47.5	0.5–1.5	10.	205.	−0.01	0	0.218	0.009	−0.096	−0.2	0.038
5*	40.0–45.0	0.5–1.5	10.	205.	−0.019	0	0.214	0.008	−0.094	0.198	0.041
6	27.5–32.5	0.5–2.0	10.	140.	0.007	0	0	0.001	−0.018	−0.003	−0.002
7	42.5–47.5	0.5–1.0	10.	222.	−0.038	0	−0.016	0.073	−0.062	−0.024	0.059
8	32.5–37.5	0.4–1.5	10.	10.	−0.007	0	0.026		−0.032	−0.007	0.045
9	52.5–57.5	0.12–1.0	10.	180.	−0.002	0	−0.086	0.024	−0.069	0.008	−0.008
10†	47.5–52.5	0.5–1.5	10.	182.	−0.002	0	−0.086	0.024	−0.069	0.008	−0.008
11†	57.5–62.5	0.5–1.5	10.	177.	−0.002	0	−0.086	0.024	−0.069	0.008	−0.008

*Station time corrections calculated from vertical component.
†Assume the same station time correction as event 9.
‡Station time correction calculated after seismogram was lagged 4 sec.
§No absolute time for this station. Seismogram was aligned with Station 2, then station time correction was calculated.

at about 45 sec with the expected polarization, phase velocity, and backazimuth for an *SV* wave from the source (the theoretical backazimuth is 140°). This remains the case until, at about 82 sec, a wave arrives with particle motion in the east direction, a slower phase velocity (2 km/sec) but a backazimuth rotated toward the south (170°). Just before 110 sec, another wave arrives with a similar phase velocity, but with particle motion to the NE and a backazimuth rotated even farther toward the SSW (to about 190°). The shorter-period band is equally complicated, with combinations of Love and Rayleigh waves continuing for more than 100 sec after the *S*-wave arrival, but all of these arrivals after about 80 sec propagate across the array with backazimuths that are rotated 30° to 60° toward the SSW from the expected direction. This is the opposite sense of rotation of backazimuth for late-arriving surface waves from that observed for the San Luis Potosi earthquake from the north. For this earthquake from the southeast, these late arrivals indicate a source of scattering or refraction located south to southwest of the array. Again, we see no significant arrivals from the east.

Another interesting earthquake was a shallow event (depth 1.5 km, magnitude 4.2) that occurred beneath the volcanics southeast of Texcoco lake (see Fig. 2), whose propagation path crosses the Valley of Mexico. In the initial inspection of waveforms for this event, we found that station 6 lagged behind about 0.75 sec relative to the other stations, indicating a clock error. Station time corrections based on the assumed *P*-wave slowness accounted for this error (the correction for station 6 is 0.779 sec; see Table 3), and the results are quite good. In the 2.5- to 5-sec band (Fig. 10), *P* waves are not visible, an *SH*/Love wave arrives at about 10 sec, and a variety of Love and Rayleigh waves arrive in groups over the following 100 sec. This is a very long duration of ground motion for an event located only 34 km away but is typical of the durations observed at stations within the lake zone. In this case, however, both source and

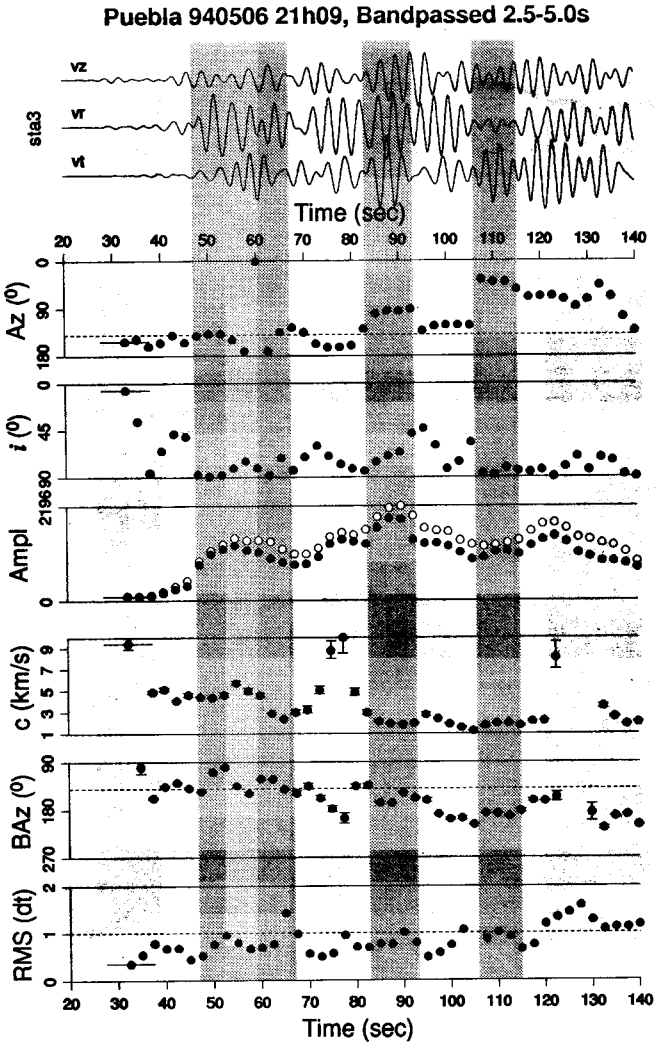

Figure 9. Array analysis results for the bandpass-filtered (2.5- to 5-sec period) ground motions from the Puebla earthquake. Same format as Figure 4.

receiver are located in the volcanics, with much of the propagation path crossing the lake zone. Following the *SH*/Love wave from about 20 to 40 sec is a Rayleigh wave with particle motion and backazimuth close to the expected direction (backazimuth 71°) and a phase velocity of 2.5 to 3 km/sec. From 40 to 60 sec is an arrival with particle motion polarized along a 100° to 120° azimuth, changing from horizontal toward vertical through time. The backazimuth for this arrival is also about 120°, rotated 50° southeast from the theoretical backazimuth, and with a slow phase velocity (1 to 2 km/sec). From about 65 to 85 sec, the phase velocity increases, and the backazimuth returns to that expected. Finally, at about 88 sec, a wave arrives with horizontal particle motion on the radial component, but with a backazimuth from the north and a very slow phase velocity. So, for the Texcoco event, at least two packets of waves cross the array with backazimuths different from the radial direction; one from the ESE and a later one from the north. It is possible that these represent internal reflections or backscattering from the same locations north and south of Mexico City that affected arrivals from the San Luis Potosi and Puebla earthquakes.

The array recorded several earthquakes from the Guerrero region of the Mexican subduction zone (see Fig. 2). These are grouped in space and time such that the recorded waveforms within each group are nearly identical. We take advantage of this multiplicity of information in interpreting the results, but we will show only one example. The three events on 4 and 5 May occurred more than 280 km from Mexico City at a backazimuth of about 200°. For all three earthquakes, the initial *P*-wave motion rapidly rotates from near vertical to horizontal, but there is little correlation between the radial components from one array station to another. Therefore, station time corrections for these events were computed using only the vertical component of the unfiltered velocity records. An example of the array analysis results (5 May, 12h18, magnitude 4.4) is shown in Figure 11. The rotation of the *P*-wave polarization is clear even in the 2.5- to 5-sec band, but the particle motion azimuth and the backazimuth are close to the expected value (205° for this event). *Lg* arrives at about 92 sec with primarily *SH* motion, although in the 1.25- to 2.5-sec band (not shown), *Lg* has a mixture of *SH* and *SV* motion. The phase velocity is about 3 km/sec, and the backazimuth (210°) is only slightly greater than the expected value. Distinct surface-wave arrivals may be identified from 130 to 155 sec, around 170 sec, and from 190 to 205 sec. In each case, the determined backazimuth is close to the expected value with, perhaps, a slight rotation to the south through time. Thus, although the very long duration of ground motion due to earthquakes in the Guerrero region indicates significant scattering, since the determined backazimuths were not significantly different than the theoretical value, this must represent forward scattering with little evidence for multipathing along the path from Guerrero.

Array recordings were also analyzed for two small earthquakes from the southwest, an offshore event in the NW

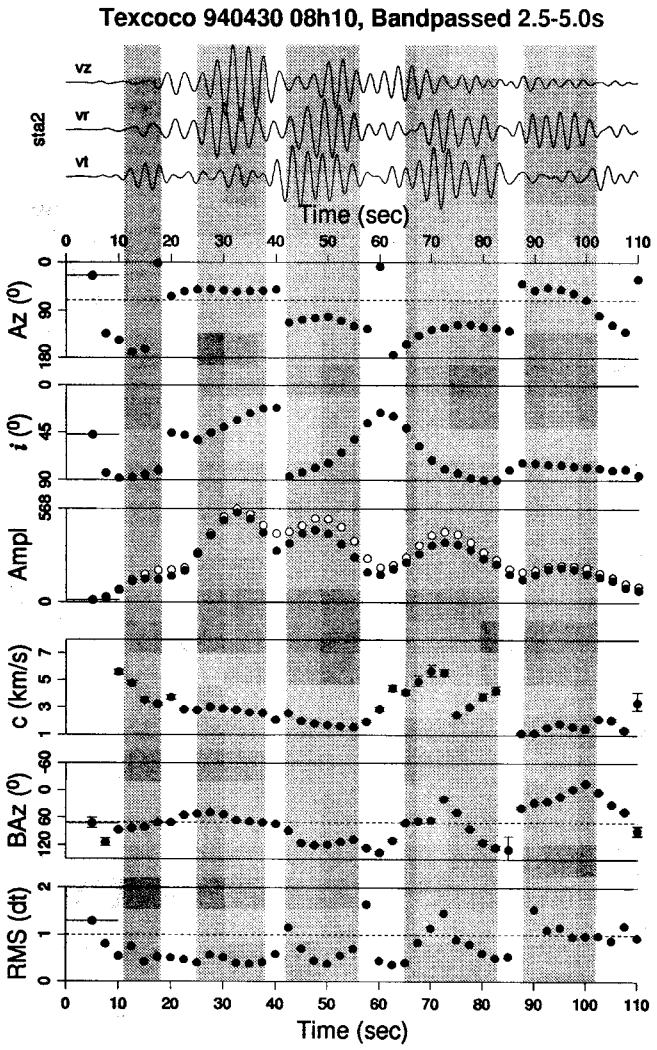

Figure 10. Array analysis results for the bandpass-filtered (2.5- to 5-sec period) ground motions from the Texcoco earthquake. Same format as Figure 4.

end of the Guerrero seismic zone on 10 May and a deep (69 km) event on-shore beneath Alto Rio Balsas. In each case, the waveforms are quite complicated, the array analysis results are highly variable, and the RMS errors are large. Therefore, it is difficult to draw conclusions regarding wave propagation along the path into Mexico City from the southwest other than to say that it may be quite complicated. Campillo *et al.* (1989) found no evidence of multipathing in their analysis of strong-motion data in Mexico City from the 1985 Michoacan earthquake.

Discussion and Conclusions

Previous studies of earthquake ground motions in the Valley of Mexico have relied on the analysis of and comparisons between individual stations. Amplification and long duration of ground motion has been documented, and mod-

els have been developed to explain these effects. However, only with a seismic array can the direction and phase velocity of interfering arrivals be distinguished within the incident wave field. The dense array of seismometers operated in the botanical garden at UNAM during April and May 1994 produced the first set of data capable of providing this information. The slow surface velocities at the array require a refined approach to array analysis, with the capability of measuring arrival-time differences between stations of less than the sampling interval of the data. Applying the method to principal-component seismograms and computing station time corrections for an assumed incident P wave provide good results for frequencies in the range of interest for seismic hazard in Mexico City.

We may draw several conclusions from these results and speculate on a cause. The initial P and Lg arrivals, which consist of waves that propagate through the entire crust, reflecting from the Moho one or more times, cross the array with the expected backazimuth. Thus, we see no evidence for laterally varying structure in the crust below the upper few kilometers. On the other hand, surface waves in the 2.5- to 5-sec band, which are sensitive to upper-crustal structure, show systematic rotations of backazimuth. Shapiro *et al.* (1996) measured the group velocities of broadband regional surface waves along a N–S profile from the coast through the Valley of Mexico. For periods of interest to this study (2 to 5 sec), they found group velocities of about 2.2 km/sec both north and south of the valley, and about 1.4 km/sec in the region immediately surrounding the valley. The southern limit coincides approximately with the southern boundary of the trans-Mexican volcanic belt (TMVB, see Fig. 12), while the northern limit falls within the TMVB near Teotihuacan. As shown in Figure 12, active volcanos (open triangles) occur in the southern portion of the TMVB, while the northern section consists of older, inactive volcanos (solid triangles) and calderas (circles). Shapiro *et al.* (1996) model the southern TMVB as an irregular 2-km-thick layer of low-velocity volcanic rock overlying the higher-velocity sedimentary rock found both north and south of the TMVB.

If we assume that the transition from fast sedimentary rock to slow volcanic rock is the source of scattering or refraction of the late, low-frequency surface waves observed at the Jardin array, since we know the backazimuth and time delay of these waves, we can back-project them to map out these sources. For example, for the San Luis Potosi event, the long-period Rayleigh wave arrives at about 90 sec with the predicted backazimuth. If we divide the path into fast and slow sections at 19.65 °N (estimated from Shapiro *et*

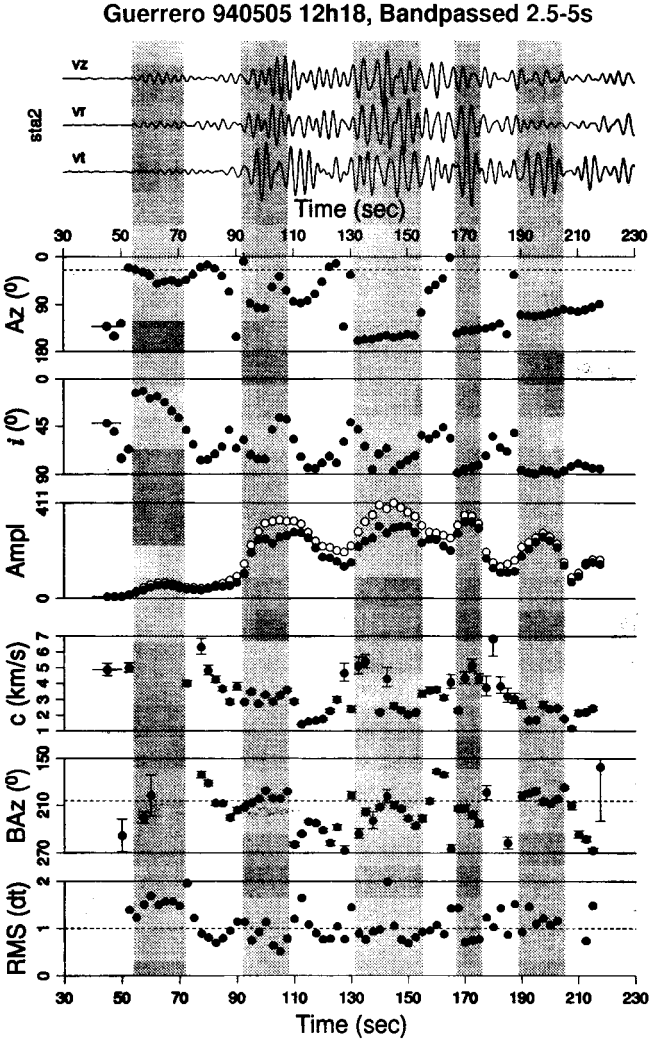

Figure 11. Array analysis results for the band-pass-filtered (2.5- to 5-sec period) ground motions from the 5 May (12h18) Guerrero earthquake. Same format as Figure 4.

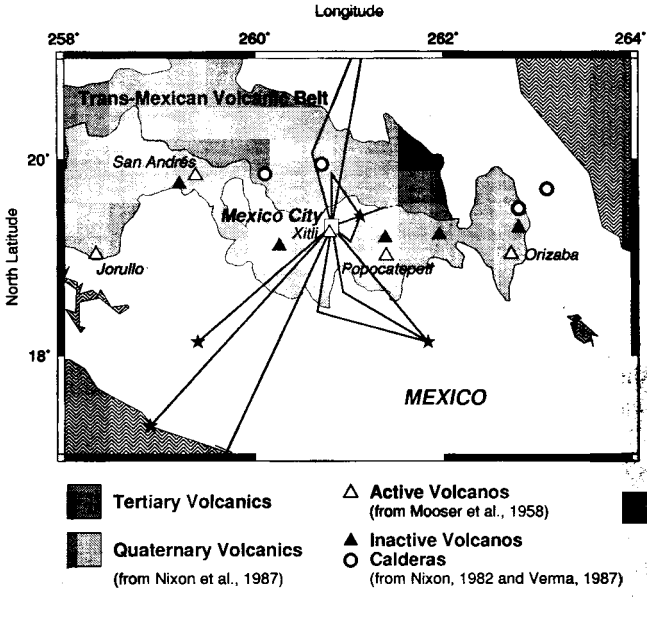

Figure 12. Map of the trans-Mexican volcanic belt (TMVB) showing inferred paths of low-frequency Rayleigh waves into the Valley of Mexico. Stars indicate earthquake epicenters. Straight lines show the "direct" raypath to the array (white square), while bent lines show scattered paths determined by back-projection.

al., 1996), this arrival time requires a group velocity of 1.5 km/sec within the volcanics and 3.0 km/sec outside (slightly faster than the results of Shapiro *et al.*, 1996). By 110 sec, the backazimuth of the long-period Rayleigh wave has rotated 25° toward the NNW. Back-projecting along this direction, we find that the time delay requires 85 km of path in the slower material and 162 km in the faster material (the latter required to close the resulting triangle). This location is near the Huichapan caldera (Verma, 1987), as shown by the bent path in Figure 12. Similarly, back-projecting the late arrivals from the Puebla earthquake, assuming the transition from fast to slow velocity for the "direct" Rayleigh wave occurs at 18.90 °N (once again estimated from Shapiro *et al.*, 1996), the two late arrivals at 85 and 106 sec result in two sources at different backazimuths. These locations correspond well with the southern margin of the TMVB (Fig. 12). For the Texcoco earthquake, the group velocity of the direct Rayleigh wave is 1.4 km/sec (in agreement with Shapiro *et al.*, 1996), and we assume that the three later arrivals represent internal reflections or scattering, so that all of the propagation is at the same group velocity. The first, from the SE, appears to originate 27.5 km from the array, within the southern TMVB at the southern margin of the Valley of Mexico near Sierra Chichinautzin. The second, which arrives on-azimuth, could be generated by very slow surface waves in the lake zone pumping energy out into the hill zone, but we have seen no evidence for this from other events. So, let us assume that it represents reflection or backscattering from a source ENE of the earthquake. Our back-projection indicates a distance of 64 km from the array, which puts the source within the N–S-trending line of volcanos that includes Popocatepetl and Iztaccihuatl near Sierra de Rio Frio. Finally, back-projection of the third late arrival indicates a source to the north at a distance of 62.5 km from the array. This may, once again, represent scattering from the vicinity of the Huichapan caldera (Fig. 12), or the surface wave may have followed the SW path of the first late arrival, then reflected or scattered a second time near the northern edge of the Valley of Mexico (near the Sierras de Tezontlalpan), before propagating southward to the array.

The array analysis for earthquakes from the Guerrero subduction zone and an on-shore earthquake southwest of Mexico City indicates no clear evidence of off-azimuth arrivals beyond the variability expected in the presence of noise. This is perhaps not surprising, since if the geometry of the TMVB at depth is reflected by its surface expression, the raypaths from these events are nearly perpendicular to the southern boundary (see Fig. 12). Several late arrivals are observed for these events, indicating significant scattering along the path. Without resorting to extremely low velocities or multiple scattering, our simple back-projection interpretation requires that the sources of scattering be located well outside of the TMVB.

For all of the earthquakes located outside of the Valley of Mexico, no significant energy was observed propagating across the array with backazimuths to the east (from the lake zone). Thus, although it is clear from amplification studies that waves resonate within the shallow sediments of the lake zone, the array analysis indicates that very little, if any, of this energy is transmitted into the hill zone where the array was located. However, long-duration ground motions are observed at the array, with evidence of multipathing for some directions of approach. The variations in backazimuth from the expected direction occur at times when coherent arrivals are observed in the seismograms and persist over several time windows, suggesting single forward scattering from structural boundaries in the upper crust. The late arrival times of these off-azimuth arrivals suggests that the source of scattering is located well beyond the Valley of Mexico and may be associated with the boundaries of the trans-Mexican volcanic belt. This would appear to support the conclusion of Singh and Ordaz (1993) that long-duration ground motions are observed in the hill zone of Mexico City resulting from scattering and multipathing between the source and the Valley of Mexico.

Acknowledgments

The Jardin array was installed and maintained with the enthusiastic help of M. A. Arreguin, R. Avila-Carrera, J. M. Castillo, D. Demanet, R. Guiguet, C. Horrent, A. Paul, N. Shapiro, M. Suarez, J. Ramos-Martinez, J. L. Rodriguez-Zuniga, and E. Romero-Jimenez. To all of them our thanks. We appreciate the logistical help of V. Caldino and R. B. Boettler of the Institute of Biology, UNAM, and of B. Sapina and F. Camacho. We thank A. Paul and O. Coutant for help in the processing of the data, and the two anonymous reviewers and associate editor Dave Wald for very helpful comments on the text. This research was supported by the Commission of the European Communities under Contracts CI1*-CT92-0025 and CI1*-CT92-0036, and with partial support from the Direccion General de Asuntos del Personal Academico, UNAM, under Grant IN108295, and from Secretaria General de Obras del DDF. The LITHOSCOPE Project was funded by CNRS/INSU. The array processing was done while J. Barker was a visiting scientist at LGIT in Grenoble with partial support from CNRS and from the U.S. Geological Survey (USGS), Department of the Interior, under USGS Award Number 1434-93-G-2277. The views and conclusions contained in this document are those of the authors and should not be interpreted as necessarily representing the official policies, either expressed or impled, of the U.S. Government.

References

Baez, G., J. Flores, J. L. Mateos, R. A. Mendez, O. Novaro, and T. H. Seligman (1994). Comment on "The origin of long coda observed in the lake-bed strong-motion records of Mexico City" by Shri Krishna Singh and Mario Ordaz, *Bull. Seism. Soc. Am.* **84,** 2015–2018.

Bard, P.-Y., M. Campillo, F. J. Chavez-Garcia, and F. Sanchez-Sesma (1988). The Mexico earthquake of September 19, 1985—a theoretical investigation of large- and small-scale amplification effects in the Mexico City valley, *Earthquake Spectra* **4,** 609–633.

Bard, P.-Y. and F. J. Chavez-Garcia (1993). On the decoupling of surficial sediments from surrounding geology at Mexico City, *Bull. Seism. Soc. Am.* **83,** 1979–1991.

Barker, J. S. (1984). A seismological analysis of the May 1980 Mammoth Lakes, California, earthquakes, *Ph.D. Dissertation,* Pennsylvania State University, University Park.

Bockelmann, G. H. R. (1995). P-wave array polarization analysis and effective anisotropy of the brittle crust, *Geophys. J. Int.* **120,** 145–162.

Campillo, M., P.-Y. Bard, F. Nicollin, and F. Sanchez-Sesma (1988). The Mexico earthquake of September 19, 1985—the incident wavefield in Mexico City during the great Michoacan earthquake and its interaction with the deep basin, *Earthquake Spectra* **4,** 591–608.

Campillo, M., J. C. Gariel, K. Aki, and F. J. Sanchez-Sesma (1989). Destructive strong ground motion in Mexico City: source, path and site effects during great 1985 Michoacan earthquake, *Bull. Seism. Soc. Am.* **79,** 1718–1735.

Campillo, M., D. Jongmans, and F. Sanchez-Sesma (1994). The influence of shallow stratigraphy on long duration ground motions in Mexico City basin: experiments and modelling, 2nd Scientific Report, Commission of the European Communities, December 1994.

Chavez-Garcia, F. J. and P.-Y. Bard (1994). Site effects in Mexico City eight years after the September 1985 Michoacan earthquakes, *Soil Dyn. Earthquake Eng.* **13,** 229–247.

Flores, J., O. Novaro, and T. H. Seligman (1987). Possible resonance effects in the distribution of earthquake damage in Mexico City, *Nature* **326,** 783–785.

Frankel, A., S. Hough, P. Friberg, and R. Busby (1991). Observation of Loma Prieta aftershocks from a dense array in Sunnyvale, California, *Bull. Seism. Soc. Am.* **81,** 1900–1922.

Hartzell, S. H., D. L. Carver, and K. W. King (1994). Initial investigation of site and topographic effects at Robinwood Ridge, California, *Bull. Seism. Soc. Am.* **84,** 1336–1349.

Jurkevics, A. (1988). Polarization analysis of three-component array data, *Bull. Seism. Soc. Am.* **78,** 1725–1743.

Kawase, H. and K. Aki (1989). A study of the response of a soft basin for incident S, P and Rayleigh waves with special reference to the long duration observed in Mexico City, *Bull. Seism. Soc. Am.* **79,** 1361–1382.

Lee, W. H. K., R. A. White, D. H. Harlow, J. A. Rogers, P. Spudich, and D. A. Dodge (1994). Digital seismograms of selected aftershocks of the Northridge earthquake recorded by a dense seismic array on February 11, 1994 at Cedar Hill Nursery in Tarzana, California, *U.S. Geol. Surv. Open-File Rept. 94-234.*

Mateos, J. L., J. Flores, O. Novaro, T. H. Seligman, and J. M. Alvarez-Tostado (1993). Resonant response models for the Valley of Mexico—II. The trapping of horizontal P waves, *Geophys. J. Int.* **113,** 449–462.

Mori, J., F. Filson, E. Cranswick, R. Borcherdt, R. Amirbekian, V. Aharonian, and L. Hachverdian (1994). Near-surface measurements of P- and S-wave velocities from the dense three-dimensional array at Garni, Armenia, *Bull. Seism. Soc. Am.* **84,** 1089–1096.

Mooser, F., H. Meyer-Abich, and A. R. McBirney (1958). *Catalogue of the Active Volcanos of the World, VI Central America,* I.V.A., Naples, 146 pp.

Nixon, G. T. (1982). The relationship between Quaternary volcanism in central Mexico and the seismicity and structure of subducted ocean lithosphere, *Geol. Soc. Am. Bull.* **93,** 514–523.

Nixon, G. T., A. Dement, R. L. Armstrong, and J. E. Harakal (1987). K-Ar and geologic data bearing on the age and evolution of the Trans-Mexican Volcanic Belt, *Geophys. Int.* **26,** (1), 109–158.

Ordaz, M. and S. K. Singh (1992). Source spectra and spectral attenuation of seismic waves from Mexican earthquakes, and evidence of amplification in the hill zone of Mexico City, *Bull. Seism. Soc. Am.* **82,** 24–43.

Pedersen, H., M. Campillo, and F. Sanchez-Sesma (1995). Azimuth dependent wave amplification in alluvial valleys, *Soil Dyn. Earthquake Eng.* **14,** 289–300.

Poupinet, G., W. L. Ellsworth, and J. Frechet (1984). Monitoring velocity variations in the crust using earthquake doublets: an application to the Caleveras fault, California, *J. Geophys. Res.* **89,** 5719–5731.

Poupinet, G., F. Moreau, M. Vadell, and D. Hatzfeld (1990). Seismic recorders and PC programs developed for the LITHOSCOPE project, *Proc. XXII General Assembly, European Seismological Commission, Barcelona,* 79–82.

Sanchez-Sesma, F. J., S. Chavez-Perez, M. Suarez, M. A. Bravo, and L. E. Perez-Rocha (1988). The Mexico earthquake of September 19, 1985—on the seismic response of the Valley of Mexico, *Earthquake Spectra* **4,** 569–589.

Sanchez-Sesma, F., M. Campillo, P.-Y. Bard, J. C. Gariel, and K. Aki (1989). The great 1985 Michoacan earthquake: a unified approach considering source, path and site effects, in *Engineering Seismology and Site Response,* A. S. Cakmak and I. Herrera, (Editors), Computational Mechanics Publ., Boston, 53–75.

Sanchez-Sesma, F. J. and F. Luzon (1996). Can horizontal *P* waves be trapped and resonate in a shallow sedimentary basin?, *Geophys. J. Int.* **124,** 209–214.

Seligman, T. H., J. M. Alvarez-Tostado, J. L. Mateos, J. Flores, and O. Novaro (1989). Resonant response models for the Valley of Mexico—I. The elastic inclusion approach, *Geophys. J. Int.* **99,** 789–799.

Shapiro, N. M., M. Campillo, A. Paul, S. K. Singh, D. Jongmans, and F. J. Sanchez-Sesma (1996). On the origin of the long period seismic amplification in the region of Mexico City, submitted to *Geophys. J. Int.*

Singh, S. K., J. Lermo, T. Dominguez, M. Ordaz, J. M. Espinosa, E. Mena, and R. Quaas (1988). The Mexico earthquake of September 19, 1985—a study of amplification of seismic waves in the Valley of Mexico with respect to a hill zone site, *Earthquake Spectra* **4,** 653–673.

Singh, S. K., R. Quaas, M. Ordaz, F. Mooser, D. Almora, M. Torres, and R. Vasquez (1995). Is there truly a "hard" rock site in the Valley of Mexico?, *Geophys. Res. Lett.* **22,** 481–484.

Singh, S. K. and M. Ordaz (1993). On the origin of long coda observed in the lake-bed strong-motion records of Mexico City, *Bull. Seism. Soc. Am.* **83,** 1298–1306.

Spudich, P., M. Hellweg, and W. H. K. Lee (1996). Directional topographic site response at Tarzana observed in aftershocks of the 1994 Northridge, California, earthquake: implications for main shock motions, *Bull. Seism. Soc. Am.* **86,** S193–S208.

Verma, S. P. (1987). Mexican Volcanic Belt: present state of knowledge and unsolved problems, *Geophys. Int.* **26** (2), 309–340.

Department of Geological Sciences and Environmental Studies
State University of New York
Binghamton, New York 13902-6000
barker@sunquakes.geol.binghamton.edu
(J.S.B.)

Laboratoire de Géophysique Interne et Tectonophysique
UA CNRS 733, B.P. 53x
Université Joseph Fourier
38041 Grenoble Cedex, France
(M.C., J.S.B.)

Instituto de Ingeniería
Universidad Nacional Autónoma de México, C.U.
Coyoacán 04510, México D.F., Mexico
and Centro de Investifacion Sismica, A.C.
Carr. al Ajusco 203, Col. H. de Padierna
Tlalpan 14200, Mexico D.F., Mexico
(F.J.S.-S.)

Laboratoire de Géologie de l'Ingénieur et d'Hydrogéologie
Université de Liége
Liége, Belgium
(D.J.)

Instituto de Geofísica
Universidad Nacional Autónoma de México, C.U.
Coyoacán 04510 México DF, Mexico
(S.K.S.)

Manuscript received 8 September 1995.